

State-of-the-art dynamic analysis for non-linear gas turbine structures

E P Petrov* and D J Ewins

Centre of Vibration Engineering, Mechanical Engineering Department, Imperial College of Science, Technology and Medicine, London, UK

Abstract: An accurate and robust method has been developed for the general multiharmonic analysis of forced periodic vibrations of bladed discs subjected to abrupt changes of elastic and damping properties at contact nodes located on the interfaces of the components. The approach is based on an analytical formulation of friction contact interface elements which provides exact expressions for multiharmonic forces and stiffness matrices of the elements. The analytical formulation overcomes the numerical difficulties associated with searching for a solution of the non-linear equations, which have been inherent so far for the considered systems, and provides a breakthrough in the analysis of the non-linear forced response of bladed discs and other structures with gaps and friction interfaces. An effective reduction method is reported that allows the size of the resolving equations to be decreased to the number of DOFs (degrees of freedom) at the contact surfaces, while preserving completeness and accuracy of the whole large-scale model.

Numerical investigations demonstrate the outstanding properties of the proposed approach with respect to computational speed, accuracy and stability of calculations for practical gas-turbine structures.

Keywords: friction contact, non-linear vibration, multiharmonic, damping

NOTATION

$\mathcal{A}_j = \mathcal{Z}_j^{-1}$	forced response function matrix for the j th harmonic
f_x, f_y	tangential and normal components of interaction forces at a friction interface
F_j^c, F_j^s	vectors of the coefficients for non-linear interaction forces
$i\mathbf{Z}(\omega)$	multiharmonic dynamic stiffness matrix
k_t, k_n	contact stiffness coefficients due to roughness of a contact surface
$\mathbf{K}, \mathbf{C}, \mathbf{M}$	stiffness, viscous damping and mass matrices
P_j^c, P_j^s	vectors of the coefficients for excitation loads
$q(t)$	vector of displacements
Q_j^c, Q_j^s	vectors of cosine and sine coefficients for the j th harmonic of the displacements
$\mathcal{Q}_j, \mathcal{F}_j, \mathcal{P}_j$	vectors of complex harmonic coefficients

\mathbf{R}	vector of residuals for multiharmonic non-linear equations of motion
$\mathbf{Z}_j, \mathcal{Z}_j$	real and complex dynamic stiffness matrices for the j th harmonic
μ	friction coefficient
ω	principal vibration frequency
$\omega_\gamma, \phi_\gamma$	natural frequencies and mode shapes of a linear structure

1 INTRODUCTION

Gas-turbine structures, such as bladed discs, rotor structures or casings (Fig. 1) and other machinery structures usually comprise many components that interact through contacting interfaces. In operation conditions these structures are subjected to dynamic forcing, which results in vibratory displacements. High vibratory displacements and stress levels that can cause failure can occur in such systems at resonance conditions when excitation frequencies and natural frequencies are close and when the spatial distribution of

The MS was received on 3 July 2003 and was accepted after revision for publication on 27 April 2004.

* Corresponding author: Centre of Vibration Engineering, Mechanical Engineering Department, Imperial College of Science, Technology and Medicine, London, SW7 2BX, UK.

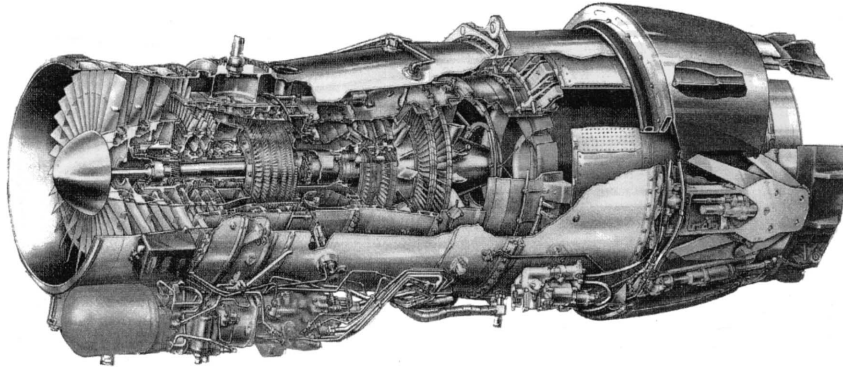


Fig. 1 A gas-turbine engine

excitation forces is similar to the deflection mode shapes of vibration of the assembly.

There are many sources of excitation in gas-turbine engines and, particularly for bladed discs where excitation forces are caused by highly inhomogeneous gas flow, these are usually a major source of vibration. Such forces can have a very dense frequency spectrum and, similarly, the spectrum of the natural frequencies of practical structures is also customarily very dense. Very dense excitation and natural frequency spectra together make the prospect of avoiding all resonance regimes almost impossible. The problem consists of developing methods and models that provide accurate, fast and robust predictive tools for the dynamic analysis of different components of gas-turbine engine structures, and especially of bladed discs, which are one of the most responsible and crucial components of the engines. Comprehensive surveys of the dynamic problems associated with bladed disc assemblies can be found in references [1] to [3].

In many practical cases forces occurring at joints and other contact interfaces of the components of an assembled structure have a significantly non-linear character. Among such primary non-linear forces are the friction forces that occur as a result of the relative motion of points of contact belonging to different components of the assembly at contact interfaces. These forces are inevitable and are usually highly beneficial because of the damping effects they produce, although the effect on surface fretting has to be taken into consideration.

Moreover, special devices, such as so-called 'friction dampers', are used in gas turbines in order to increase damping and to restrict the level of resonant vibration amplitudes. The effectiveness of using friction for damping of vibrations is very much dependent on geometry and the characteristics of contact surfaces, the parameters of components of the assembly, the choice of parameters for the friction dampers and on excitation loads. The problem of modelling friction forces for the dynamic analysis of different machinery structures is discussed in the extensive surveys of

references [4] and [5], and the friction models used for the dynamic analysis of bladed discs are considered in the review paper of reference [6]. Some more recent investigations of dynamics of the bladed discs with friction elements are described in references [7] to [13]. A variable normal load at the friction contact interface changes not only the friction force levels but also the instants of slip-stick transitions, significantly affecting the friction forces, and friction models taking into account the normal load variation have recently been developed and reported in references [14] to [17].

Another major source of non-linear contact forces are the forces of unilateral interaction at the contact interfaces. These forces permit the transmission of compression stresses but not extension and cannot generally be linearized. Furthermore, clearances and interferences at the contact surfaces are inevitable in practical assemblies and when these open and close under certain vibration conditions, they change the areas of the contact interfaces. The resulting non-linear interaction significantly affects the resonance frequencies, friction damping and forced response levels.

Non-linear forces can also change dynamic properties of structures significantly. In many cases, they cause qualitatively new phenomena that do not exist in the dynamics of linear systems. Such phenomena include multivalued forced response levels for a structure with given design parameters and excitation, sub- and super-harmonic resonances, dependence of steady state forced responses on initial values of displacements and velocities of the structure, etc. Special methods have to be developed to solve the resulting non-linear equations of motion numerically. From the point of view of temporal behaviour, problems occurring in gas turbine dynamics can be divided into (a) a class of non-periodic, transient dynamics non-linear problems and (b) a class of periodic, steady state vibration. The latter problem usually prevails in practical forced response analysis and among the most effective methods for calculation of the periodic solution are the multiharmonic balance methods, which permit effective accounting for periodicity of the sought solution and the avoidance of having to

undertake time integration of the equations of motion. When non-linear effects are significant, the customary principle of superposition is no longer valid and the harmonic components of vibration displacements cannot be analysed separately. These harmonic components of the response displacement interact through non-linear interface forces and several of them can occur simultaneously even when a mono-harmonic excitation is applied. For the common practical case of multi-harmonic excitation, interaction of different harmonics can affect the response levels significantly. Some formulations and applications of the multiharmonic balance methods to the non-linear dynamics problem are presented in references [18] to [25].

Notwithstanding the many investigations that there have been of the dynamic behaviour of structures with friction contact interfaces, the problem of developing efficient and robust methods for the analysis of multi-harmonic forced response levels of practical structures, using large-scale finite element models, still needs to be solved. In this paper, new reliable and efficient computational models and a robust method to provide a prediction of response levels of such structures developed recently by the authors are reported.

Friction contact interface elements are described by allowing for variable normal load and for the existence of clearances and interferences. The friction interface elements used describe unilateral contact along the normal to a contact surface and the friction forces under the variable normal load. No restrictions on the level of the normal load variation are imposed, which allows the model to be used for the practically inevitable cases when separation of the contact surfaces occurs under vibration conditions.

To guarantee high accuracy and rapid convergence of the iterative solution process, the non-linear interface elements are derived analytically, including derivation of their tangent stiffness matrix for multiharmonic vibration analysis. The resulting expressions allow the interaction forces and the stiffness matrix to be calculated with the accuracy of the real number presentation in the computer, while providing extremely fast calculation of the characteristics of the contact interaction. The accuracy of the analytical derivation overcomes common difficulties encountered in numerical analysis of non-linear structures comprising interfaces with abrupt changes of contact conditions (such as contact/absence of contact, slip/stick, etc.). Such difficulties have been inherent so far and in many cases they have even caused a loss of convergence and failure to find a solution.

A method for analysing primary non-linear vibrations of structures using large-scale finite element (FE) models is elaborated in this paper. A multiharmonic balance formulation for the equations of motion is derived and a method to reduce the size of the resulting non-linear equations is proposed, which preserves the accuracy of the initial model.

The outstanding efficiency of the method is demonstrated in a set of representative test cases, including (a) some using large FE models of practical bladed discs with friction dampers and where impacts between shrouds are considered and (b) a model of a test piece for an impact damper test rig.

2 PROBLEM FORMULATION

The equation for the forced response of a non-linear structure consisting of a linear part, which is independent of vibration amplitude, and non-linear friction interfaces can be written in the following form:

$$\mathbf{K}\mathbf{q}(t) + \mathbf{C}\dot{\mathbf{q}}(t) + \mathbf{M}\ddot{\mathbf{q}}(t) + \mathbf{f}(\mathbf{q}(t), \dot{\mathbf{q}}(t)) - \mathbf{p}(t) = \mathbf{0} \quad (1)$$

where \mathbf{K} , \mathbf{C} and \mathbf{M} are the stiffness, viscous damping and mass matrices respectively of its linear part, which can include terms corresponding to the action of centrifugal, Coriolis, thermoelastic and other linear static forces; $\mathbf{p}(t)$ is a vector of external periodic excitation forces with a known period, T .

In equation (1), $\mathbf{q}(t)$ is a vector of nodal displacements for all the degrees of freedom (DOFs) in the structure considered. The vector, $\mathbf{q}(t)$, comprises a vector of 'linear DOFs', \mathbf{q}^{lin} , and a vector of 'non-linear DOFs' (i.e. DOFs at interfaces where interaction forces with non-linear dependence on displacements can occur at some instants or over time intervals), \mathbf{q}^{nl} . The non-linear DOFs include all those nodes of the FE models where the non-linear forces can act and also the nodes where non-linear interactions might occur. Under dynamic loading, clearances in the structure can be closed and interferences can be opened up and, as a result, contact areas can vary during vibration (see Fig. 2). The nodes where non-linear forces act in reality are determined as a result of calculation, and the vector, \mathbf{q}^{nl} , usually has a larger number of DOFs than the number of nodes where non-linear effects occur. In the majority of practical structures, the number of linear DOFs is much larger than the number of non-linear DOFs.

The term $\mathbf{f}(\mathbf{q}(t), \dot{\mathbf{q}}(t))$ is a vector of non-linear friction interface forces which are dependent on the displace-

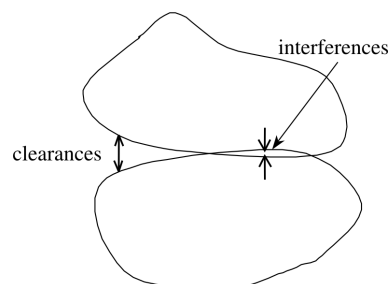


Fig. 2 A friction contact interface

ments and velocities of the interacting nodes. Models of the non-linear forces occurring at the friction contact interfaces describe forces of unilateral contact along a direction normal to the contact surface and friction forces acting in directions that are tangential to the contact surface. The effects of variations in the normal load on the friction force are modelled, including the case of partial separation of the contact surfaces. The models of the contact forces include provision of initial values of clearances and interferences as parameters.

3 METHOD OF CALCULATION

3.1 Transformation of equations of motion to the frequency domain using the multiharmonic balance method

Steady state, periodic regimes of vibration response are sought and a vector of forced response, $q(t)$, satisfying equation (1) is determined. In order to search for a periodic vibration response, the variation of all DOFs of the system in time is represented as a restricted Fourier series, which can contain as many and such harmonic components as are necessary to approximate the sought solution with a desired accuracy, i.e.

$$q(t) = Q_0 + \sum_{j=1}^n Q_j^c \cos m_j \omega t + Q_j^s \sin m_j \omega t \quad (2)$$

where n is a number of harmonics kept in the multiharmonic solution, Q_0 , Q_j^c and Q_j^s ($j = 1, \dots, n$) are vectors of harmonic coefficients for the system DOFs, m_j ($j = 1, \dots, n$) are specific harmonics that are kept in the displacement expansion in addition to the constant component and ω is the fundamental vibration frequency.

The fundamental frequency is defined by a period of the sought vibration response. In an analysis of vibration gas-turbine structures for most practical cases, major resonance regimes (i.e. when the period of the forced response is equal to the period of excitation forces) are the subject of interest. The fundamental frequency is determined for this case to be $\omega = 2\pi/T$. The multiharmonic representation of the forced response allows superharmonic resonances to be determined along with major resonances. For cases when subharmonic vibrations (i.e. when the period of vibration is a multiple of the period of excitation forces, $j_1 T$, where $j_1 > 1$ is an integer number) or combination resonance regimes (i.e. when the period of vibration is equal to $j_1 T/j_2$, where j_1 and j_2 are integer numbers) need to be determined, the fundamental frequency can relate to the period of excitation forces in the following way: $\omega = 2\pi/(j_1 T/j_2)$.

In accordance with the multiharmonic balance method, the expansion from equation (2) is substituted into equation (1), after which it is sequentially multiplied

by $(\cos m_j \omega)$ and $(\sin m_j \omega)$ to reveal all the harmonics from the expansion from which the integrals over the vibration period are calculated. As a result, equations for determining all the harmonic components are obtained in the form

$$Z(\omega)Q + F(Q) - P = 0 \quad (3)$$

where $Q = \{Q_0, Q_1^c, Q_1^s, \dots, Q_n^c, Q_n^s\}^T$ is a vector of harmonic coefficients for the system, $F(Q)$ is a vector of non-linear forces, P is a vector of harmonic components of exciting forces and $Z(\omega)$ is the dynamic stiffness matrix of the linear part of the system, constructed for all harmonic components, i.e.

$$Z = \text{diag}[Z_0, Z_{m_1}, \dots, Z_{m_n}] \quad (4)$$

where

$$Z_0 = K \quad \text{and} \quad Z_j = \begin{bmatrix} K - (m_j \omega)^2 M & m_j \omega C \\ -m_j \omega C & K - (m_j \omega)^2 M \end{bmatrix} \quad (5)$$

Although matrix Z is block-diagonal, equation (3) represents a set of simultaneous non-linear equations with respect to Q because the equations for all harmonic components are coupled through the vector of non-linear forces, $F(Q)$, which is dependent on all harmonic components of the displacements.

3.2 Condensation and size reduction for the non-linear equations of motion

Finite element models of practical gas-turbine structures, and even models of the individual components, usually comprise very many degrees of freedom; indeed, hundreds of thousands or millions of DOFs in the models are customary in such industrial applications. The number of governing equations is equal to the number of DOFs multiplied by the number of harmonic coefficients in the multiharmonic expansion. The large number of simultaneous non-linear equations thus obtained cannot be solved directly due to the size of the matrices involved and prohibitively high computational expense. In order to make the analysis of a non-linear forced response feasible for such large systems, a special effective reduction technique has been developed. This technique reduces the number of DOFs explicitly retained in the resolving non-linear equations to the number of non-linear DOFs, i.e. to those where non-linear forces are applied. All the other, linear, DOFs are excluded from the reduced equations while the accuracy of the description of the dynamic properties of the structure is preserved. After determination of the non-linear DOFs at the non-linear contact interfaces, the displacements at any node of interest in the whole large-scale FE model can then be easily determined.

In order to perform this reduction efficiently, it is convenient to rewrite equation (3) using complex arithmetic. Such a formulation allows the relationships to be reduced immediately by a factor of two and is useful for further reduction. In order to make such a formulation, complex vectors for each of the j th harmonic vectors of complex displacements, \mathcal{Q}_j , non-linear forces, \mathcal{F}_j , and excitation forces, \mathcal{P}_j , are introduced in the following form:

$$\begin{aligned} \mathcal{Q}_j &= \mathbf{Q}_j^c + i\mathbf{Q}_j^s, & \mathcal{P}_j &= \mathbf{P}_j^c + i\mathbf{P}_j^s, \\ \mathcal{F}_j &= \mathbf{F}_j^c + i\mathbf{F}_j^s \end{aligned} \quad (6)$$

where $i = \sqrt{-1}$ and all the complex quantities are written here and further in the paper using a different font in order to differentiate them from their real counterparts. A complex dynamic stiffness matrix for each j th harmonics, \mathcal{L}_j , is introduced as

$$\mathcal{L}_j = [\mathbf{K} - (m_j\omega)^2\mathbf{M}] - im_j\omega\mathbf{C} \quad (7)$$

Equation (3) can now be rewritten separately for each of the j th harmonics, taking into account the block diagonal structure of the dynamic stiffness matrix, \mathbf{Z} , in the following form:

$$\begin{aligned} \mathcal{L}_j\mathcal{Q}_j + \mathcal{F}_j(\mathbf{Q}) - \mathcal{P}_j &= \mathcal{Q}_j + \mathcal{L}_j^{-1}(\mathcal{F}_j(\mathbf{Q}) - \mathcal{P}_j) \\ &= \mathcal{Q}_j + \mathcal{A}_j(\mathcal{F}_j(\mathbf{Q}) - \mathcal{P}_j) \\ &= \mathbf{0} \quad (j = \overline{0, n}) \end{aligned} \quad (8)$$

Here $\mathcal{A}_j = \mathcal{L}_j^{-1}(\omega)$ is an FRF matrix of a linear structure determined for a case when non-linear interaction forces are not applied. In order to avoid the numerically inefficient operation of matrix inversion, the FRF matrix can be efficiently generated from the natural frequencies, ω_γ , and mode shapes, ϕ_γ , of this linear structure:

$$\mathcal{A}_j = \mathcal{L}_j^{-1}(\omega) \simeq \sum_{\gamma=1}^{N_m} \frac{\phi_\gamma\phi_\gamma^T}{(1 - i\eta_\gamma)\omega_\gamma^2 - \omega^2} \quad (9)$$

Here the subscript γ is the number of the mode shape in the spectrum, η_γ is the damping loss factor determined for the γ th mode and N_m is the number of modes that are used in the modal expansion. In many cases, relatively small numbers of modes, N_m , need to be kept in the expansion to provide sufficient accuracy in the FRF matrix calculation (analysis of the accuracy obtained for FRF matrices of bladed disc models is performed in reference [26]).

In order to derive equations with excluded linear DOFs, the vector of complex amplitudes for the j th harmonic, \mathcal{Q}_j , is partitioned into a vector of non-linear DOFs, $\mathcal{Q}_j^{\text{nl}}$, and a vector of linear DOFs, $\mathcal{Q}_j^{\text{lin}}$, i.e. $\mathcal{Q}_j = \{\mathcal{Q}_j^{\text{lin}}, \mathcal{Q}_j^{\text{nl}}\}^T$, and then equation (8) can be

rewritten in the form

$$\left\{ \begin{matrix} \mathcal{Q}_j^{\text{lin}} \\ \mathcal{Q}_j^{\text{nl}} \end{matrix} \right\} + \left\{ \mathcal{A}_j^{\text{nl}} \mathbf{0} \right\} - \mathcal{A}_j\mathcal{P}_j = \mathbf{0} \quad (10)$$

where $\mathcal{A}_j^{\text{nl}}$ is a minor of matrix \mathcal{A}_j , corresponding to the non-linear DOFs, and \mathcal{Q}^{nl} is a subset of vector \mathcal{Q} , which contains all the harmonic coefficients of displacements at the non-linear interfaces. Selecting from equation (10) those equations that correspond to the non-linear DOFs, the required equation of significantly reduced size is

$$\mathcal{R}_j(\mathcal{Q}^{\text{nl}}) = \mathcal{Q}_j^{\text{nl}} + \mathcal{A}_j^{\text{nl}}\mathcal{F}_j(\mathcal{Q}^{\text{nl}}) - \mathcal{P}_j^{\text{nl}} = \mathbf{0} \quad (11)$$

where $\mathcal{Q}_j^{\text{nl}}$ is a vector of complex amplitudes for the j th harmonic and $\mathcal{P}_j^{\text{nl}} = (\mathcal{A}_j\mathcal{P}_j)^{\text{nl}}$ is a vector of complex amplitudes determined for the non-linear DOFs when the non-linear forces appearing at the contact interfaces of the analysed structure are not taken into account. The vector of excitation forces, $\tilde{\mathcal{P}}_j$, can include forces applied to all DOFs of the structure, linear as well as non-linear. The FRF matrix including all the DOFs, \mathcal{A}_j , is used to evaluate vector, $\mathcal{A}_j\mathcal{P}_j$, and then the components that correspond to the non-linear DOFs are selected from the resulting vector to form $\mathcal{P}_j^{\text{nl}}$. When the solution of equation (11) is found, the forced response for all DOFs, \mathcal{Q}_j , is easily determined from Eq. (8).

Equations of form (11) formulated for all the harmonics of the multiharmonic expansion are non-linear. Owing to the dependence of the non-linear contact interface forces on all these harmonics, they have to be solved simultaneously. One of the most effective methods for the solution of non-linear equations is the Newton–Raphson method. The iterative solution process can be expressed by the following formula:

$$\mathbf{Q}^{(k+1)} = \mathbf{Q}^{(k)} + \left(\frac{\partial \mathbf{R}}{\partial \mathbf{Q}} \right)^{-1} \mathbf{R}(\mathbf{Q}^{(k)}) \quad (12)$$

where

$$\mathbf{R} = \{\mathbf{R}_0, \text{Re}(\mathcal{R}_1), \text{Im}(\mathcal{R}_1), \dots, \text{Re}(\mathcal{R}_{m_n}), \text{Im}(\mathcal{R}_{m_n})\}^T$$

is a real vector of residuals of the non-linear equations (11). The superscript (k) indicates the number of iterations and the superscript nl is dropped here. It can be seen that a non-linear force vector, $\mathbf{F}(\mathcal{Q}^{\text{nl}})$, and a tangent stiffness matrix, $\mathbf{K}(\mathcal{Q}^{\text{nl}}) = \partial \mathbf{F}(\mathcal{Q}^{\text{nl}}) / \partial \mathcal{Q}^{\text{nl}}$, which is included in $\partial \mathbf{R} / \partial \mathbf{Q}$, have to be provided to apply this method. It should be noticed that transforming the equation in real arithmetic is a necessary requirement in order to apply the Newton–Raphson method. This requirement occurs due to the fact that generally $\mathcal{R}_j(\mathcal{Q})$ cannot be expressed as an analytic function of the complex vector \mathcal{Q} and hence derivatives $\partial \mathcal{R}^{(k)} / \partial \mathcal{Q}$ are not determined for complex arithmetic.

3.3 Friction contact interface elements

When the derivatives $\partial F(\mathbf{Q})/\partial \mathbf{Q}$ are calculated using finite difference formulae, this results in (a) a very large computational effort, (b) difficulty with the choice of the step for the numerical evaluation of the derivatives and, very often, (c) a loss of accuracy and robustness of the solution. To overcome these problems, analytical expressions have been derived for a non-linear force vector of the friction contact interfaces, $\mathbf{F}(\mathbf{Q})$, and for its tangent stiffness matrix, $\partial \mathbf{F}(\mathbf{Q})/\partial \mathbf{Q}$. The expressions derived allow exact and extremely fast calculations to be made for the contact interaction forces and tangent stiffness matrices as functions of displacements of the contacting components of the structure. This, in turn, results in outstanding robustness and speed of the forced response calculations for the analysed structure.

As an example of the analytical derivation for contact interface elements, a friction contact element that models friction forces acting along a direction tangential to the contact surface as well as unilateral forces (i.e. transferring compression but not tension) acting along the normal direction have been described. Distribution of such elements over areas where nodes of the finite element mesh can come into contact allows the forced response to be calculated for a structure accounting for variable contact areas, multiple slip–stick transitions during periods of multiharmonic vibration and friction impacts at contact–separation transitions. A friction model applied in this paper takes into account the effects of variations in normal load on friction forces. These effects include not only variations of the friction force magnitude but also the influence of the normal load variation on time instants when stick–slip transitions occur. These transition times can be different from times when the direction of motion is changing.

During relative motion of the contacting surfaces with friction, several different states are possible. The motion along the normal direction, $y(\tau)$, determines whether the interacting surfaces are in contact or separated. When the surfaces are in contact then two other different states are possible: slip or stick depending on the tangential motion, $x(\tau)$, normal motion, $y(\tau)$, and the history of the interaction. Expressions for non-linear interaction forces can be defined for all possible states in the following form:

$$\begin{aligned}
 & \text{tangential force} \\
 f_x = & \begin{cases} f_x^0 + k_t(x(\tau) - x_0) & \text{for stick} \\ \xi(\tau)\mu f_y(\tau) & \text{for slip} \\ 0 & \text{for separation} \end{cases} \\
 & \text{normal force} \\
 f_y = & \begin{cases} N_0 + k_n y(\tau) & \text{for contact} \\ 0 & \text{for separation} \end{cases}
 \end{aligned} \tag{13}$$

where $\tau = \omega t$ is non-dimensional time, the contact surface mechanical properties are described by a friction coefficient, μ , and the stiffness coefficients for deformation along tangential and normal directions to the contact surface, k_t and k_n , and $\xi(\tau) = \pm 1$ is a sign function of the tangential force at the time instant of slip state initiation, τ_{slip} . For the conventional case of a constant normal force, the value of the sign is determined by that of the tangential velocity: $\xi = \text{sgn}[\dot{x}(\tau_{\text{slip}})]$. However, for the case of a variable normal load, considered here, the sign is dependent on mutual action of the normal load and the tangential velocity on the time of slip–stick transitions. It does not necessarily coincide with the direction of the relative motion. To guarantee time continuity of the tangential force the sign function is determined by that of the tangential force at the end of the preceding stick phase, i.e. $\xi = \text{sgn}[f_x(\tau_{\text{slip}})]$.

The times of transitions, τ_j , between all possible states of the contact interaction are determined from the following conditions:

$$\begin{aligned}
 |f_x(\tau)| = \mu f_y(\tau) & & \text{for stick–slip transition} \\
 \dot{\xi} f_x(\tau) = \mu \dot{f}_y(\tau) \text{ and } \xi \ddot{f}_x(\tau) < \mu \ddot{f}_y(\tau) & & \text{for slip–stick transition} \\
 f_y(\tau) = 0 \text{ and } \dot{f}_y(\tau) < 0 & & \text{for contact–separation transition} \\
 f_y(\tau) = 0 \text{ and } \dot{f}_y(\tau) > 0 & & \text{for separation–contact transition}
 \end{aligned} \tag{14}$$

where one or two dots above the symbols denote first or second time derivatives, and the expression from equations (13) corresponding to the contact state is used for the normal load, $f_y(\tau)$.

A more detailed description of the friction model is given in reference [16] and the effects of the variations of normal load and other contact parameters on friction forces are demonstrated in reference [17].

Multiharmonic motion of each degree of freedom is expressed in the following form: $x(\tau) = \mathbf{H}_-^T(\tau)\mathbf{X}$, $y(\tau) = \mathbf{H}_-^T(\tau)\mathbf{Y}$, where \mathbf{X} and \mathbf{Y} are vectors of harmonic coefficients of the relative motion of the mating contact nodes in the tangential and normal directions respectively and $\mathbf{H}_- = \{1, \cos m_1\tau, \sin m_1\tau, \dots, \cos m_n\tau, \sin m_n\tau\}^T$. Vectors of multiharmonic Fourier expansion coefficients for tangential, \mathbf{F}_x , and normal, \mathbf{F}_y , forces can be obtained in the form

$$\begin{aligned}
 \begin{Bmatrix} \mathbf{F}_x \\ \mathbf{F}_y \end{Bmatrix} &= \frac{1}{\pi} \sum_{j=1}^{n_\tau} \int_{\tau_j}^{\tau_{j+1}} \begin{Bmatrix} \mathbf{H}_+(\tau) f_x \\ \mathbf{H}_+(\tau) f_y \end{Bmatrix} d\tau \\
 &= \sum_{j=1}^{n_\tau} \begin{Bmatrix} \mathbf{J}_x^{(j)} \\ \mathbf{J}_y^{(j)} \end{Bmatrix}
 \end{aligned} \tag{15}$$

where

$$\mathbf{H}_+ = \{1/2, \cos m_1\tau, \sin m_1\tau, \dots, \cos m_n\tau, \sin m_n\tau\}^T.$$

Substitution of the expressions for the interaction forces given by equations (13) into equation (15) gives an expression for the force vector. Introduced here are vectors of integrals $\mathbf{J}_x^{(j)}$ and $\mathbf{J}_y^{(j)}$ over each interval of stick, slip or separation, which are obtained in the form

$$\mathbf{J}_x^{(j)} = \begin{cases} k_t \mathbf{W}_j \mathbf{X} + c_j \mathbf{w}_j & \text{stick} \\ \xi \mu (N_0 \mathbf{w}_j + k_n \mathbf{W}_j \mathbf{Y}) & \text{slip} \\ \mathbf{0} & \text{separation} \end{cases}$$

$$\mathbf{J}_y^{(j)} = \begin{cases} N_0 \mathbf{w}_j + k_n \mathbf{W}_j \mathbf{Y} & \text{contact} \\ \mathbf{0} & \text{separation} \end{cases} \tag{16}$$

where

$$c_j = f_x^0(\tau_j) - k_{x,x}(\tau_j) = -\xi \mu (N_0 + k_{n,y}(\tau_j)) - k_{t,x}(\tau_j)$$

$$\mathbf{W}_j = \frac{1}{\pi} \int_{\tau_j}^{\tau_{j+1}} \mathbf{H}_+(\tau) \mathbf{H}_-^T(\tau) d\tau$$

$(n \times n)$

and $\mathbf{w}_j = \frac{1}{\pi} \int_{\tau_j}^{\tau_{j+1}} \mathbf{H}_+(\tau) d\tau$

$(n \times 1)$

(17)

The stiffness matrix of the friction interface element is determined by differentiating equation (15) with respect to vectors \mathbf{X} and \mathbf{Y} . Because of the independence of the normal force to the tangential displacement, the stiffness matrix has the following, inherently unsymmetrical, structure:

$$\mathbf{K}_f = \begin{bmatrix} \frac{\partial \mathbf{F}_x}{\partial \mathbf{X}} & \frac{\partial \mathbf{F}_x}{\partial \mathbf{Y}} \\ \mathbf{0} & \frac{\partial \mathbf{F}_y}{\partial \mathbf{Y}} \end{bmatrix} = \sum_{j=1}^{n_\tau} \begin{bmatrix} \frac{\partial \mathbf{J}_x^{(j)}}{\partial \mathbf{X}} & \frac{\partial \mathbf{J}_x^{(j)}}{\partial \mathbf{Y}} \\ \mathbf{0} & \frac{\partial \mathbf{J}_y^{(j)}}{\partial \mathbf{Y}} \end{bmatrix} \tag{18}$$

where

$$\frac{\partial \mathbf{J}_x^{(j)}}{\partial \mathbf{X}} = \begin{cases} k_n \mathbf{W}_j + \mathbf{w}_j \left(\frac{\partial c_j}{\partial \mathbf{X}} \right)^T & \text{stick} \\ \mathbf{0} & \text{slip} \\ \mathbf{0} & \text{separation} \end{cases}$$

$$\frac{\partial \mathbf{J}_x^{(j)}}{\partial \mathbf{Y}} = \begin{cases} \mathbf{w}_j \left(\frac{\partial c_j}{\partial \mathbf{Y}} \right)^T & \text{stick} \\ \xi \mu k_n \mathbf{W}_j & \text{slip} \\ \mathbf{0} & \text{separation} \end{cases}$$

$$\frac{\partial \mathbf{J}_y^{(j)}}{\partial \mathbf{Y}} = \begin{cases} k_n \mathbf{W}_j & \text{contact} \\ \mathbf{0} & \text{separation} \end{cases} \tag{19}$$

Since the vector used for the transformation from the time domain into the frequency domain, \mathbf{H}_+ , and that for transformation backwards, \mathbf{H}_- , consists of sine and cosine functions of different orders, then components of matrix \mathbf{W} and vector \mathbf{w} are simple integrals of sine and cosine functions and integrals of products of these

functions. These integrals can be calculated analytically, thus providing an exact and very fast calculation for the vectors of the Fourier expansion coefficients of the interface forces and the stiffness matrix.

The stiffness coefficients k_n and k_t characterize stiffness properties for a contact point of the layer of microasperities that are inherent owing to inevitable roughness of the contact surfaces. The multitude of friction contact elements that developed when distributed over an FE mesh of the structure can model contact areas that are varied during vibration, including a description of closing and opening interferences and clearances. Hence many different realistic friction interactions can be modelled with a detailed description of contact conditions and geometry of the contact surfaces.

4 NUMERICAL RESULTS

The method developed has been realized in a program suite FORSE (standing for ‘forced response suite’) and is applied to analysis of realistic bladed discs used in the gas-turbine industry, providing good agreement with experimental measurements.

4.1 A practical high-pressure turbine bladed disc

As an example of application, the friction contact interface elements reported above have been applied for the analysis of the vibration response of a practical high-pressure bladed turbine disc comprising 92 blades. A finite element model of the sector of the bladed disc is shown in Fig. 3a. It contains more than 160 000 DOFs and the whole bladed disc is described by more than 15 million DOFs. The damping loss factor of the bladed disc without friction dampers included is 0.003. Natural frequencies of the high-pressure turbine disc are shown in Fig. 3b for all possible nodal diameter numbers. A case when there are no underplatform damper and blade shroud friction contacts, i.e. non-linear interaction forces, are not applied and the system is linear with blades interacting through the disc. The natural frequencies are normalized with respect to the first blade-alone frequency. Cyclic symmetry properties of the structure considered were introduced into the analysis of the non-linear vibration behaviour using a method developed in reference [27].

4.1.1 Tuned bladed disc with underplatform friction dampers

For an analysis of the influence of friction dampers on the forced response of the bladed disc, the nodes where each of the bladed disc sectors has a friction contact,

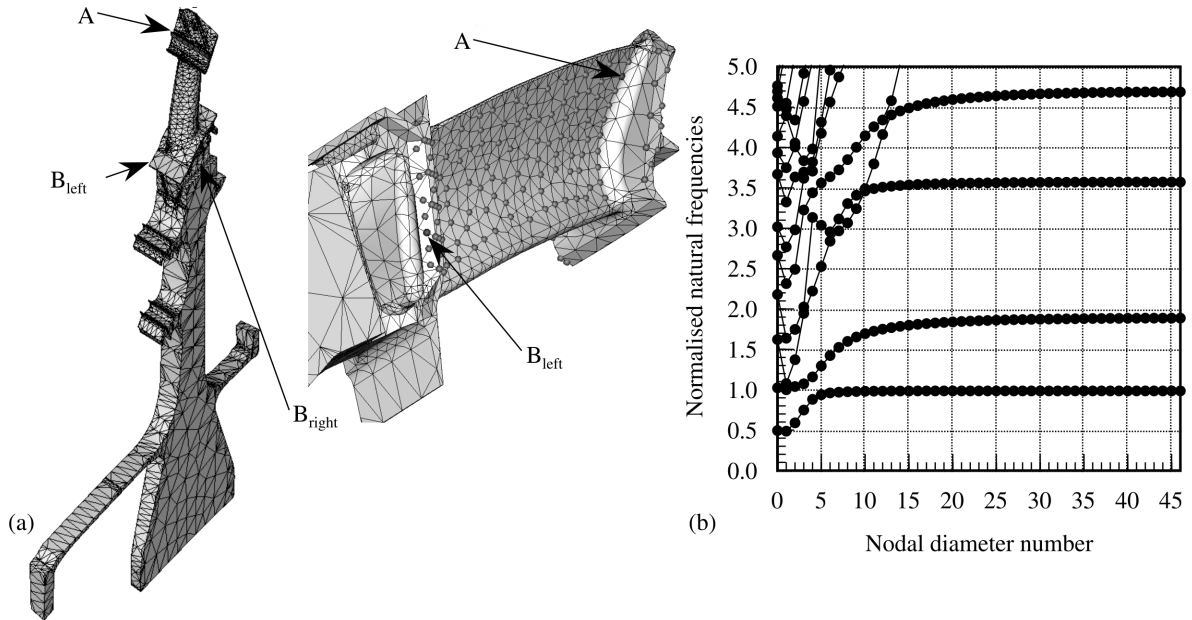


Fig. 3 Finite element model of a sector of the turbine bladed disc and nodes of friction contact

marked as B_{left} and B_{right} in Fig. 3a, are located at the blade platform. Another node, A, where displacements are calculated is selected near the tip of the blade. These nodes are marked in Fig. 3a by circles. For each sector, node B interacts through the friction element with the corresponding node of the adjacent sector of the bladed disc and its counterpart on the other, left-hand, side of the considered sector interacts with the preceding sector. As an example, forcing by 4th, 6th, 8th and 16th engine order excitations are considered in the frequency range corresponding to the family of first predominantly flap-wise blade modes and in the frequency range of the

second family of natural frequencies. In order to compare the damping effect produced by the friction elements, the amplitudes of the excitation loads are assumed to be the same for all engine orders studied.

Examples of maximum response levels for displacement at a node A are shown in Fig. 4 where, for comparison, response levels for the bladed disc without the friction damper are also plotted. Damping produced by the friction dampers decreases the response amplitudes significantly and, moreover, the friction damper can be seen to increase the resonance frequency significantly. For both the considered families of modes

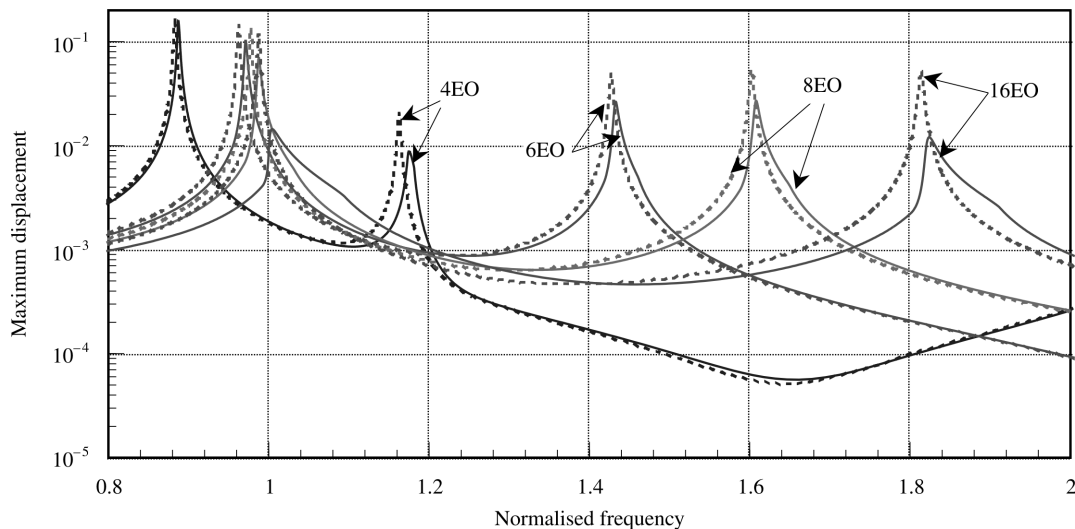


Fig. 4 Forced response of the high-pressure turbine bladed disc with a friction damper (solid line) and without a friction damper (dashed line) for different numbers of engine orders

(first flap-wise modes and first edge-wise modes with different numbers of nodal diameters), greater damping effects appear for the higher engine orders when the relative displacements of neighbouring blades are largest. In all these calculations faultless determination of the solution with accuracy $\|\mathbf{R}(\mathbf{Q})\| < 10^{-8}$ was obtained, and for each curve calculated for Fig. 4 over a whole range from 800 to 3200 Hz, only 60 seconds of CPU (central processing unit) time was required on a personal computer with 450 MHz CPU frequency.

4.1.2 The bladed disc with contacting shrouds

The forced response of the same bladed disc was analysed when contact of integral shrouds was considered to be possible (Fig. 5). Two cases of contact interaction are explored: (a) the case when each shroud can contact its neighbours at one node (this node is marked by the letter A in Fig. 5b at the left-hand-side contact interface); (b) the case when many nodes distributed over the shroud contact faces can be in contact with the adjoining shrouds (marked by the letter B in Fig. 5b). Different values of gap between the shrouds are considered, namely: (a) a case of interference, i.e. negative gap values: $g = -0.001$; (b) a case of zero gaps: $g = 0.0$; and (c) a case of positive gap values: $g = 0.001$. The forced response was calculated at the same node as for the case of the bladed disc with friction dampers (see the node marked by a letter A in Fig. 3a) and excitation by the fourth engine order (4EO) is examined.

Results of the calculations for all the considered cases are shown in Fig. 6, where, for comparison, forced responses of the bladed disc for the case of linear vibrations are plotted alongside (a) forced response of the bladed disc when shrouds never contact and (b) forced response of the bladed disc when contact nodes are always in full contact. It can be seen that for the shrouds with clearances, the forced response in the frequency ranges where the amplitudes

are smaller than these clearances coincides with the forced response of the bladed disc without contact. For larger amplitude levels the system exhibits forced response characteristic ‘stiffening’ with an amplitude increase. For the shrouds with interferences the forced response in frequency ranges where amplitudes are smaller than the interferences coincides with the response of the bladed disc with full contact, and for larger amplitude levels the system exhibits a ‘softening’ of the forced response curve. For cases with multiple-contact nodes non-linear behaviour starts at a lower level of response and the resonance frequency can vary over much larger ranges than for a case of single-node contact. This effect is especially significant for a case of clearances. For the case of zero gaps, the forced response differs from that of the linear system compared over the whole frequency range analysed. For this case, resonance frequencies differ significantly, although neither stiffening nor softening of the resonance curves occurs. To calculate the forced response over the whole excitation frequency range, from 20 to 360 seconds of CPU time was required, depending on the number of contact nodes and the complexity of the forced response curve.

The influence of structural damping on the forced response curves was also analysed, and an example of results obtained for the case of multiple node contact and for two different values of the structural damping, $\eta = 0.003$ and $\eta = 0.02$, is shown in Fig. 7 for the case of the gap equal to 0.001. Here it can be seen that a sufficient level of damping for this strongly non-linear system has two favourable effects: (a) similar to the case of linear vibration, it reduces the level of resonance amplitudes and (b) it also reduces drastically the frequency range where the resonances (which depend on amplitude for the non-linear system) can be excited: e.g. instead of the frequency range 1.15, ..., 2.2, where the second resonance can occur for a case of $\eta = 0.003$, for larger damping, $\eta = 0.02$, a relatively high level of amplitudes exhibits only in the small vicinity of frequency 1.15.

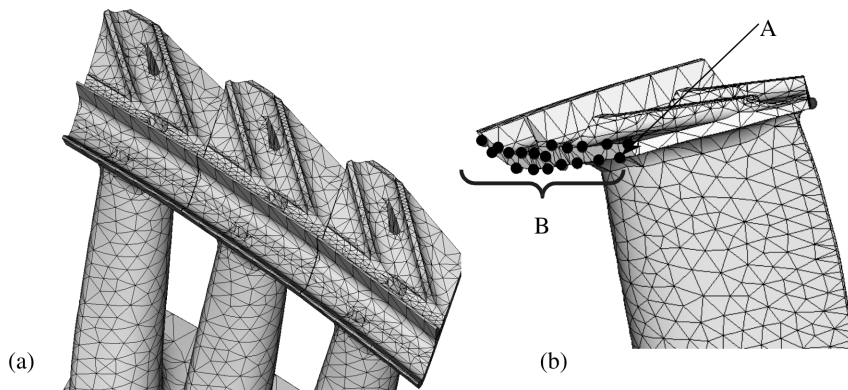


Fig. 5 Integral shroud model and nodes of possible contact considered in the calculations

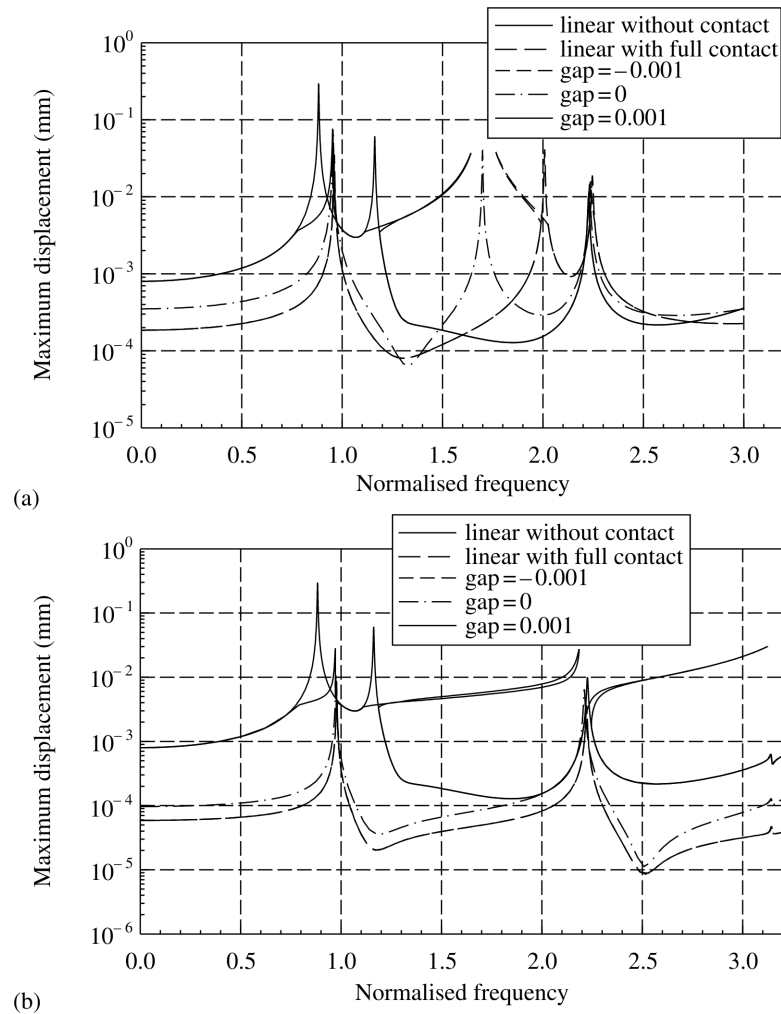


Fig. 6 Forced response of the high-pressure turbine bladed disc: (a) shrouds have a single contact node; (b) shrouds interact through many contact nodes

4.2 Impact damper test piece

The capabilities available by using the gap elements developed above for the analysis of structures with impact dampers were explored on the example of a test

piece of an impact damper test rig. The test piece consists of a beam and an impact damper placed in a chamber made within the brick (Fig. 8). The beam and the impact damper are both modelled using solid finite elements and a finite element model of the test piece

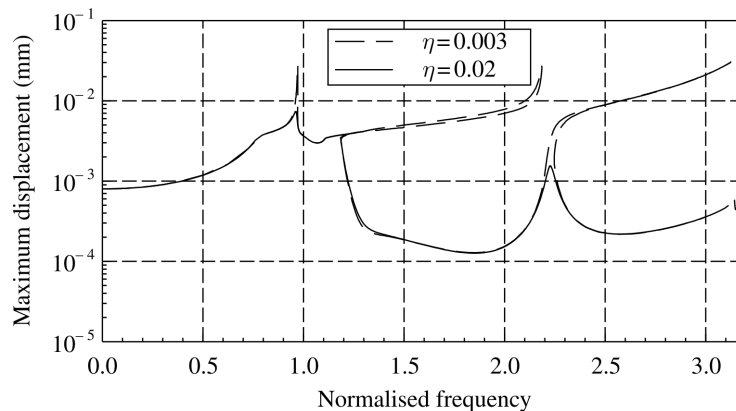


Fig. 7 Forced response of the turbine bladed disc for different levels of structural damping

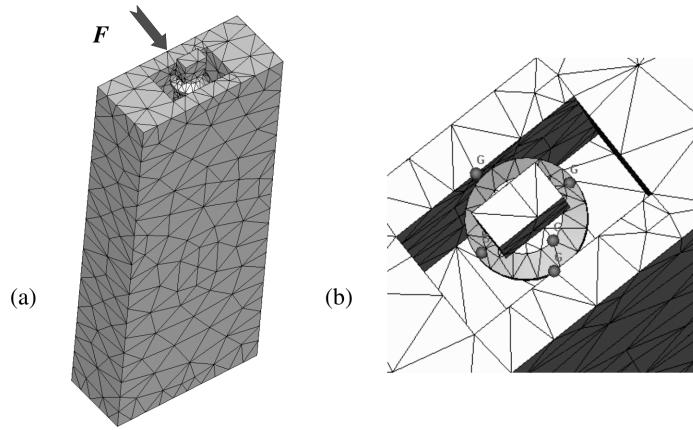


Fig. 8 Impact damper test rig: (a) finite element model of the test piece; (b) the impact damper

consists of more than 96 000 DOFs. The beam is clamped at one end and vibrations are excited by a force applied at the other end, with proportional structural damping assumed to be 0.0016. Friction damping and energy dissipation due to inelastic deformation at impacts are neglected and unilateral interaction of the damper and the brick during vibration is modelled by the gap elements only. The possibilities of reducing the maximum forced response level by varying the impact damper parameters (gaps, contact stiffness coefficient, mass) were explored. It was found that mass variation was the most effective parameter in the practically imposed restrictions on the parameter values.

Examples of calculated forced responses for three impact damper configurations are shown in Fig. 9. These three different impact dampers (A, B and C) have relative mass values $m_A < m_B < m_C$, and the gaps between the walls of the internal brick chamber and the impact damper are 0.2 mm in all cases. For reference, the forced response of the beam without the impact damper, i.e. when vibrations are linear, is also shown. It can be seen that the proper choice of parameters for the impact damper can reduce resonance amplitudes significantly, although use of such an impact

damper device can increase the level of amplitudes that are far from resonances. In contrast to the linear system, the introduction of the impact damper makes the forced response curves multivalued. The choice of which branch of the calculated forced response to follow in practice depends on the direction of the excitation frequency sweep and on perturbations of displacements and velocities for the beam and the friction damper. It was found that 20 seconds of CPU time were required to calculate the forced response over the whole frequency range considered in Fig. 9 for each case of the damper design.

5 CONCLUDING REMARKS

A new method has been developed for the analysis of the steady state non-linear vibration response of a gas-turbine engine and other machinery structures with joints and friction contacts. The method developed enables extremely fast and robust calculations to be made of multiharmonic forced responses for a wide range of problems occurring in the dynamics of complex

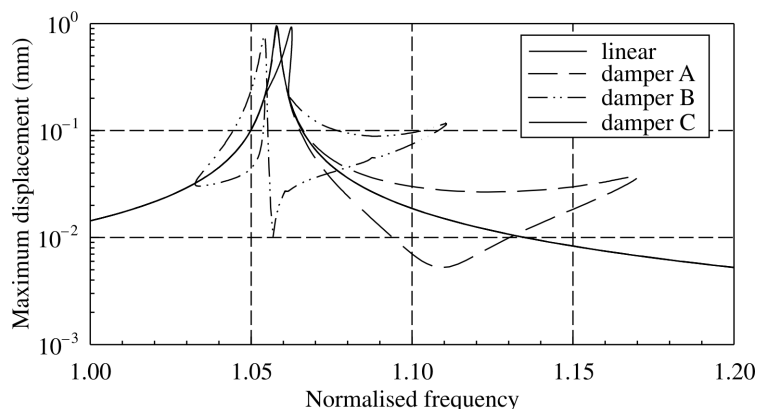


Fig. 9 Forced responses of the impact damper test rig for impact dampers of different masses

structures using large-scale finite element models. The method offers the possibility for a breakthrough in the analysis of non-linear forced responses of structures with gaps and friction.

The friction model developed takes into account the effects of normal load variations of an arbitrary level, including separation of contact surfaces on friction forces. Analytical formulation of the friction contact elements provides exact expressions for the contact forces and stiffness matrices of the contact interface and allows fast and robust calculations to be made for the non-linear forced responses.

The high efficiency of the method is demonstrated using examples of calculations for practical bladed discs with friction and impacts and on specially selected test cases. Finite element models with large numbers of degrees of freedom and with multiple friction and impact contact nodes were analysed.

ACKNOWLEDGEMENT

The authors are grateful to Rolls-Royce plc for providing the financial support for this project and for giving permission to publish this work.

REFERENCES

- 1 **Ewins, D. J.** Vibration characteristics of bladed disc assemblies. *J. Mech. Engng Sci.*, 1973, **15**(3), 165–186.
- 2 **Srinivasan, A. V.** Flutter and resonant vibration characteristics of engine blades. *Trans. ASME, J. Engng for Gas Turbines and Power*, 1997, **119**, 742–775.
- 3 **Slater, J. C., Minkiewicz, G. R. and Blair, A. J.** Forced response of bladed disk assemblies—a survey. *Shock and Vibr. Dig.*, 1999, **31**(1), 17–24.
- 4 **Ibrahim, R. A.** Friction-induced vibration, chatter, squeal, and chaos. Part I: mechanics of contact and friction; Part II: dynamics and modeling. *Trans. ASME, Appl. Mechanics Rev.*, 1994, **47**, 209–226 (Part I), 227–253 (Part II).
- 5 **Armstrong-Helouvry, B., Dupont, P. and de Wit, C. C. A.** A survey of models, analysis tools and compensation methods for the control of machines with friction. *Automatica*, 1994, **30**, 1083–1138.
- 6 **Griffin, J. H.** A review of friction damping of turbine blade vibration. *Int. J. Turbo and Jet Engines*, 1990, **7**, 297–307.
- 7 **Sextro, W.** The calculation of the forced response of shrouded blades with friction contacts and its experimental verification. In Proceedings of 2nd European Nonlinear Oscillation Conference, Prague, Czech Republic, 9–13 September 1996.
- 8 **Griffin, J. H., Wu, W.-T. and El-Aini, Y.** Friction damping of hollow airfoils: Part I—theoretical development. *Trans. ASME, J. Engng for Gas Turbines and Power*, 1998, **120**, 120–125.
- 9 **Csaba, G.** Forced response analysis in time and frequency domain of a tuned bladed disc with friction dampers. *J. Sound Vibr.*, 1998, **214**(3), 395–412.
- 10 **Yang, B. D. and Menq, C. H.** Characterization of contact kinematics and application to the design of wedge dampers in turbomachinery blading. Part 1: stick–slip contact kinematics; Part 2: prediction of forced response and experimental verification. *Trans. ASME, J. Engng for Gas Turbines and Power*, 1998, **120**, 410–417 (Part 1), 418–423 (Part 2).
- 11 **Csaba, G.** Modelling of a microslip friction damper subjected to translation and rotation. ASME paper 99-GT-149, 1999.
- 12 **Szwedowicz, J., Kissel, M., Ravindra, B. and Kellerer, R.** Estimation of contact stiffness and its role in the design of a friction damper. In Proceedings of ASME Turbo Expo 2001, New Orleans, 4–7 June paper 2001, 2001-GT-0290.
- 13 **Sanliturk, K. Y., Ewins, D. J. and Stanbridge, A. B.** Underplatform dampers for turbine blades: theoretical modelling, analysis and comparison with experimental data. *Trans. ASME, J. Engng for Gas Turbines and Power*, 2001, **123**, 919–929.
- 14 **Yang, B. D., Chu, M. I. and Menq, C. H.** Stick–slip–separation analysis and non-linear stiffness and damping characterization of friction contacts having variable normal load. *J. Sound Vibr.*, 1998, **210**(4), 461–481.
- 15 **Yang, B. D. and Menq, C. H.** Characterization of 3D contact kinematics and prediction of resonant response of structures having 3D frictional constraint. *J. Sound Vibr.*, 1998, **217**(5), 909–925.
- 16 **Petrov, E. P. and Ewins, D. J.** Analytical formulation of friction interface elements for analysis of nonlinear multi-harmonic vibrations of bladed discs. *Trans. ASME, J. Turbomachinery*, April 2003, **125**, 364–371.
- 17 **Petrov, E. P. and Ewins, D. J.** Generic friction models for time-domain vibration analysis of bladed discs. *Trans. ASME, J. Turbomachinery*, January 2004, **126**, 184–192.
- 18 **Pierre, C., Ferri, A. A. and Dowell, E. H.** Multi-harmonic analysis of dry friction damped systems using an incremental harmonic balance method. *Trans. ASME, J. Appl. Mechanics*, 1985, **52**, 958–964.
- 19 **Cameron, T. M. and Griffin, J. H.** An alternating frequency/time domain method for calculating steady response of nonlinear dynamic systems. *Trans. ASME, J. Appl. Mechanics*, 1989, **56**, 149–154.
- 20 **Lau, S. L. and Zhang, W. S.** Nonlinear vibrations of piecewise-linear systems by incremental harmonic balance method. *Trans. ASME, J. Appl. Mechanics*, 1992, **59**, 153–160.
- 21 **Wang, J. H. and Chen, W. K.** Investigation of the vibration of a blade with friction damper by HBM. *Trans. ASME, J. Engng for Gas Turbines and Power*, 1993, **115**, 294–299.
- 22 **Cardona, A., Coune, T., Lerusse, A. and Geradin, M.** A multiharmonic method for non-linear vibration analysis. *Int. J. Numer. Meth. Engng*, 1994, **37**, 1593–1608.
- 23 **Sanliturk, K. Y., Imregun, M. and Ewins, D. J.** Harmonic balance vibration analysis of turbine blades with friction dampers. *Trans. ASME, J. Vibr. Acoust.*, 1997, **119**, 96–103.
- 24 **Berthillier, M., Dupont, C., Mondal, R. and Barrau, R. R.** Blades forced response analysis with friction dampers. *Trans. ASME, J. Vibr. Acoust.*, 1998, **120**, 468–474.

- 25 Chen, J. J. and Menq, C. H.** Prediction of periodic response of blades having 3D nonlinear shroud constraints. ASME paper 99-GT-289, 1999, pp. 1–9.
- 26 Petrov, E. P., Sanliturk, K. Y. and Ewins, D. J.** A new method for dynamic analysis of mistuned bladed discs based on exact relationship between tuned and mistuned systems. *Trans. ASME, J. Engng for Gas Turbines and Power*, July 2002, **122**, 586–597.
- 27 Petrov, E. P.** A method for use of cyclic symmetry properties in analysis of nonlinear multiharmonic vibrations of bladed discs. *Trans. ASME, J. Turbomachinery*, January 2004, **126**, 175–183.